Mon. Not. R. Astron. Soc. **000**, 1–6 (...) Printed 1 March 2013 (MN LATEX style file v2.2)

Neutron star atmosphere composition: the quiescent, low-mass X-ray binary in the globular cluster M28

M. Servillat[1,2⋆], C. O. Heinke[3], W. C. G. Ho[4], J. E. Grindlay[1], J. Hong[1], M. van den Berg[5,1], and S. Bogdanov[6]

[1] *Harvard-Smithsonian Center for Astrophysics, 60 Garden Street, Cambridge, MA 02138, USA*
[2] *Laboratoire AIM (CEA/DSM/IRFU/SAp, CNRS, Université Paris Diderot), CEA Saclay, Bat. 709, 91191 Gif-sur-Yvette, France*
[3] *Department of Physics, University of Alberta, CCIS 4-183, Edmonton AB, T6G 2E1, Canada; Ingenuity New Faculty*
[4] *School of Mathematics, University of Southampton, Southampton, SO17 1BJ, United Kingdom*
[5] *Astronomical Institute Anton Pannekoek, University of Amsterdam, Science Park 904, 1098 XH Amsterdam, the Netherlands*
[6] *Columbia Astrophysics Laboratory, Columbia University, 550 West 120th Street, New York, NY 10027-6601, USA*

Accepted .... Received ...; in original form ...

ABSTRACT

Using deep *Chandra* observations of the globular cluster M28, we study the quiescent X-ray emission of a neutron star in a low-mass X-ray binary in order to constrain the chemical composition of the neutron star atmosphere and the equation of state of dense matter. We fit the spectrum with different neutron star atmosphere models composed of hydrogen, helium or carbon. The parameter values obtained with the carbon model are unphysical and such a model can be ruled out. Hydrogen and helium models give realistic parameter values for a neutron star, and the derived mass and radius are clearly distinct depending on the composition of the atmosphere. The hydrogen model gives masses/radii consistent with the canonical values of 1.4 $M_\odot$ and 10 km, and would allow for the presence of exotic matter inside neutron stars. On the other hand, the helium model provides solutions with higher masses/radii, consistent with the stiffest equations of state. Measurements of neutron star masses/radii by spectral fitting should consider the possibility of heavier element atmospheres, which produce larger masses/radii for the same data, unless the composition of the accretor is known independently.

Key words: equation of state – stars: neutron – globular clusters: individual (M28 or NGC 6626) – X-rays: binaries – X-rays: individual (CXOGlb J182432.8-245208)

1 INTRODUCTION

Neutron stars (NS) are composed of the densest form of matter known to exist in our Universe, providing us with a unique laboratory to study cold matter at supra-nuclear density. For example, it is still not well understood whether exotic condensates occur in the NS core. The chemical composition of the outer envelope is also uncertain, as well as the symmetry energy, the behavior of superfluidity among neutrons and protons, and the conductivity of the NS crust. Measuring the masses or radii of these objects can lead to useful constraints on the dense matter equation of state (EOS), and give insights of the composition of NSs (see Lattimer 2010 for a recent review).

Masses have been determined very accurately for a few dozen NSs in binaries containing pulsars (for a recent compilation, see Lattimer & Prakash 2010). Measured masses for a variety of NS systems range from 1.0 to 2.5 $M_\odot$, with a canonical mass of 1.4 $M_\odot$. In particular, the high NS mass measured with high precision for the pulsar PSR J1614-2230 (1.97 ± 0.04 $M_\odot$) brings doubts on the presence of hyperons or free quarks in NS interiors (Demorest et al. 2010), though those solutions are not completely ruled out (e.g. Weissenborn et al. 2011; Massot et al. 2012).

For systems in which the NS is hot enough to emit detectable X-rays from the surface, due to youth or accretion, the X-ray spectrum can be used to constrain both the radius and mass of the NS (Lattimer 2010; Özel et al. 2010; Steiner et al. 2010; Galloway & Lampe 2012). The mass and radius of isolated NS or ones in transient low-mass X-ray binaries (LMXBs) can be inferred from spectral modeling if their distances are accurately determined. In the case of accreting NS transients located in globular clusters (GCs), relatively accurate distances are known (errors of ∼5%, see e.g. Krauss & Chaboyer 2003). Even though, the uncertainties for individual NS measurements are still large

⋆ E-mail: mservillat@cfa.harvard.edu

(Rutledge et al. 2002a; Gendre et al. 2003a; Heinke et al. 2006; Webb & Barret 2007; Guillot et al. 2011), but the ensemble of observations can ultimately improve constraints on the dense matter EOS (e.g. Steiner et al. 2010).

It has been shown that the surface of a weakly magnetic ($B < 10^{10}$ G) NS should be chemically very pure and dominated by the lightest element present as the heavier elements settle out of the atmosphere within seconds to minutes (Alcock & Illarionov 1980; Brown et al. 2002). If there is accretion after the NS formation, the atmosphere could be composed of hydrogen –H– or helium –He– as heavier elements are expected to be destroyed via nuclear spallation reactions (Bildsten et al. 1992; Chang & Bildsten 2004). A fraction of the incident He also suffers spallation reactions and may reform through fusion reactions (Bildsten et al. 1993). The ratio of H to He is thus not well determined. If no accretion takes place or if all lighter elements are burned, heavy elements are expected (Chang et al. 2010, and references therein).

Different NS atmosphere models have been developed, but most recent work for low magnetic fields has focused on a pure H model, such as the ones developed by Zavlin et al. (1996), Gänsicke et al. (2002), or Heinke et al. (2006). The latter model, NSATMOS, was further developed to represent atmospheres of pure He, carbon, nitrogen, oxygen or iron (Ho & Heinke 2009). In particular, such models were used for the low magnetic field NS located at the center of the Cassiopeia A supernova remnant, which was shown to harbor a carbon atmosphere (Ho & Heinke 2009).

The GC M28 (NGC 6626) is located at a distance of $D = 5.5 \pm 0.3$ kpc (from Harris 1996, 2010, using measurements in Testa et al. 2001) at RA $= 18^h24^m32.81^s$ and Dec $= -24°52'11.2''$ (J2000). The reddening toward M28 is $E(B-V) = 0.42 \pm 0.02$ (Testa et al. 2001), implying a H column density of $N_{\rm H} = (2.33 \pm 0.12) \times 10^{21}$ cm^2 (using Predehl & Schmitt 1995 for conversion).

Becker et al. (2003) have previously reported on a set of ∼40 ks *Chandra* X-ray Observatory ACIS-S observations of M28 (ObsIds 2683, 2684, 2685). They suggested that the luminous, soft *Chandra* source numbered 26 in their work (IAU-approved source name CXOGlb J182432.8-245208) is a transiently accreting NS in a LMXB in quiescence (qLMXB). We keep the name source 26 throughout the text. Fitting its spectrum with a H atmosphere model (NSA model, Zavlin et al. 1996) yielded the effective temperature $T_\infty \sim 90$ eV and the projected radius $R_\infty \sim 14.5$ km with the mass set to 1.4 $M_\odot$, corresponding to a NS temperature $T_{\rm NS} \sim 125$ eV and radius $R_{\rm NS} \sim 10.4$ km.

In this paper we focus on this NS qLMXB in M28 using one of the deepest *Chandra* observations of a GC to date and recent atmosphere models with different chemical compositions. We present the data in Section 2, and a variability and spectral analysis in Section 3. We finally discuss the results and implications in Section 4.

2 DATA

The Chandra data set used here was already presented by Bogdanov et al. (2011). Two long observations were acquired on 2008 August 7 (ObsId 9132) and 2008 August 10 (ObsId 9133) for 144 and 55 ks, respectively (PI: J. Grindlay). We also included the three observations presented by Becker et al. (2003, ObsIds 2683, 2684, and 2685, PI: W. Becker). All observations were taken with ACIS-S in VFAINT telemetry mode, and TIMED read mode with a frame time of 3.1 s and reading time of 0.041 s. The data re-processing, reduction, and analysis were performed in the same way as presented by Bogdanov et al. (2011), but using the more recent CIAO 4.4 and CALDB 4.4.8. In particular, we did not used the back-ground cleaning algorithm specific to the VFAINT telemetry mode as this procedure tends to reject real source counts for relatively bright sources.

We used the CIAO tool wavdetect and the script PWDetect (Damiani et al. 1997) to detect source candidates in the field of view. Subsequently, we employed the IDL script ACIS Extract (Broos et al. 2010) to confirm the validity of the source detections and refine the source positions. This lead to the detection of 101 sources inside the half mass radius of M28, and 35 inside the core radius, with a minimum of 4 counts per source.

The qLMXB candidate, source 26 of Becker et al. (2003), is detected with a total of 10332 counts (∼0.043 cts s^{-1}) in the 0.3–6 keV energy band. We extracted the events of the target in a 1.25″ radius region, enclosing 95% of the total source energy for an effective energy of 1 keV. We estimated that the contamination from close-by detected sources is <1%. The background was extracted from three 24″ radius regions surrounding the GC core radius, making sure the regions are source free. The data is clean from background flares, except in ObsId 2683 where the background flux reaches 5 times its median value for 4 ks over the 14 ks observation. However, this corresponds to a negligible contamination of ∼0.5 count in the aperture of the target (0.1% of the target counts in that ObsId), we thus kept all the data in this obsid.

We used *dmextract* to extract a lightcurve with a 1000 s binning (minimum of 30 counts per bin), and *dmcopy* to extract an event list for the source and background. Using *specextract*, which includes an energy dependent aperture correction (*arfcorr*), we extracted a spectrum and generated response files for each dataset. The spectra were binned with a minimum of 50 counts to use χ^2 statistics for the fitting. We discarded bins flagged as bad, and bins below 0.3 keV where the response of the instrument is not calibrated (calibration down to 0.3 keV with ACIS-S3 has been clearly improved in CALDB 4.4[1]).

3 RESULTS

3.1 Light curve and search for variability

We show in Figure 1 the lightcurve of the target for all five observations with a 1000 s binning, as well as the median energy of the source in each bin. We report the lightcurve characteristics and variability tests in Table 1. For each lightcurve we computed the χ^2 of a fit with a constant and performed a Kolmogorov-Smirnov (KS) test of variability. The source showed no significant variability in all Chandra observations. There is no feature in the light-curve that would indicate a periodic variability, or flares, and we found

[1] http://cxc.harvard.edu/cal/memos/contam_memo.pdf

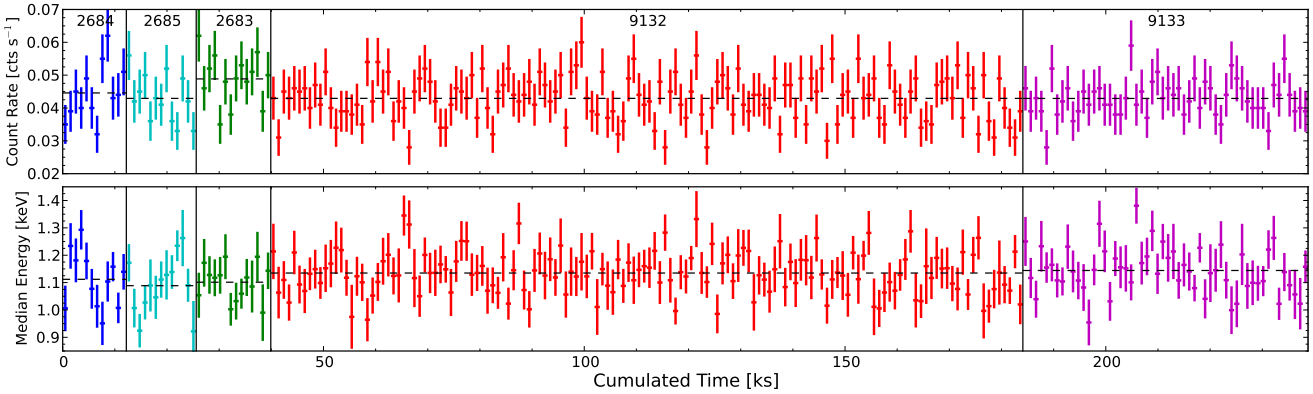

Figure 1. X-ray lightcurve of the M28 *Chandra* source 26. The five ObsIds are presented in consecutive pannels. The count rate and the median energy are calculated in the 0.3–6 keV energy band.

Table 1. Properties of the X-ray observations of the M28 *Chandra* source 26.

ObsId	Date	Exp.Time [ks]	Counts	Rate [10^{-2} c/s]	Median Energy [keV]	Mean Energy [keV]	χ^2/dof	KS prob. %	Frac. rms %
2684	2002-07-04	12.2	561	4.4±0.2	1.11±0.03	1.2±0.5	10.7/13	22	<23
2685	2002-08-04	13.4	569	4.3±0.2	1.08±0.02	1.2±0.5	12.8/14	32	<24
2683	2002-09-09	14.3	684	4.9±0.2	1.10±0.03	1.2±0.5	12.8/14	48	<21
9132	2008-08-07	144.2	6182	4.29±0.05	1.13±0.01	1.2±0.5	120.6/144	52	<12
9133	2008-08-10	54.7	2336	4.3±0.1	1.14±0.01	1.2±0.5	26.0/56	45	<21
All		238.8	10332	4.29±0.04	1.13±0.01	1.2±0.5	173.3/200	38	<11

no correlation between the flux and median energy of the source as a function of time. We also give the fractional rms (root mean square) of the light-curve. As the observed variability is consistent with noise, a 3σ limit on the fractional rms is given in Table 1.

The possible 4σ increase of flux reported for ObsId 2683 compared to 2684 and 2685 (Becker et al. 2003) is not observed in this work. The mean count rate is slightly higher (about 2σ) in observation 2683, but the scatter around the mean for this ObsId is not unusual, as can be seen in Figure 1. Similarly, we found no significant change in the mean energy. There may be an increase of the median energy between 2002 and 2008 of ∼0.03 keV, which is marginal (less than 2σ).

3.2 Spectral fitting

We fitted simultaneously the five spectra extracted from the five different epochs with Xspec 12.7.0e (Arnaud 1996), using the pure H atmosphere model NSATMOS (Heinke et al. 2006) and a photoelectric absorption $N_{\rm H}$ along the line of sight (TBABS, with abundances from Wilms et al. 2000). We first tied all parameters between the different datasets, which seems a reasonable assumption as the source did not show significant variability between the different epochs (section 3.1). We fixed the distance to 5.5 kpc and the normalization to 1 (i.e. we assume that all the NS surface is emitting). We also kept at first the mass and radius to the canonical values, 1.4 $M_\odot$ and 10 km respectively. This returned a marginally acceptable fit with a reduced χ^2 (χ^2_ν) of 1.27 and 144 degrees of freedom (dof). Data bins at energies higher than 2 keV show systematic positive residuals, mainly visible for the ObsId 9132 spectrum (see Figure 2).

Given the count rate and softness of the source, which is almost on-axis, we expect some level of pile-up in the spectrum (5% using PIMMS 4.2[2]). This effect occurs when two or more photon events overlap in a single detector frame and are being read as a single event, creating a high energy tail in a contaminated spectrum. We used the pile-up model component available in Xspec (Davis 2001) with a frame time set to 3.1 s and a free α parameter (related to the probability of events being retained as a good grade after filtering). This model gave the best fit (χ^2_ν/dof = 0.88/143), with $\alpha = 0.41 \pm 0.15$. We refitted the spectrum with the mass and radius parameters free to vary. The best fit model (χ^2_ν/dof = 0.87/141) is obtained for $N_{\rm H} = (2.5 \pm 0.3) \times 10^{21}$ cm^2, a temperature $kT_{\rm eff} = 125 \pm 40$ eV, a mass $M = 1.4^{+0.4}_{-0.9}$ $M_\odot$ and a radius $R = 9 \pm 3$ km. Errors are at 90% significance and we considered only masses higher than 0.5 $M_\odot$ and radii higher than 6 km. The 0.3–6 keV absorbed flux of the source (after removing the pile-up effect) is then $(1.8 \pm 0.2) \times 10^{-13}$ erg s^{-1} cm^{-2}, and the unabsorbed luminosity $\sim 1.6 \times 10^{33}$ erg s^{-1} (at 5.5 kpc). This spectrum is reported in Figure 2. We then ran the command *steppar* and obtained confidence contours for the mass and radius of the NS, which are more instructive than the best fit parameter values and errors (see Figure 3, left).

Though no obvious variability was found in section 3.1, we tested this assumption by untying the normalization for

[2] http://cxc.harvard.edu/toolkit/pimms.jsp

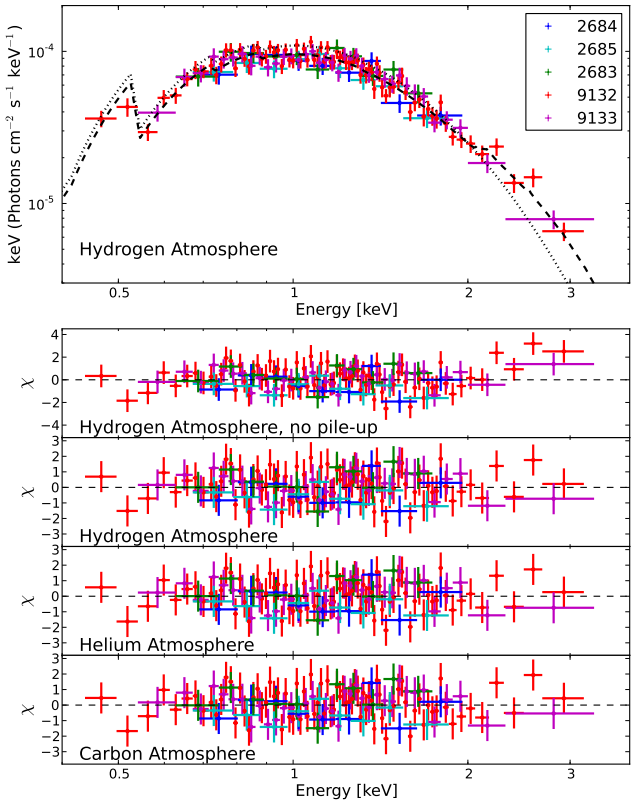

Figure 2. Spectrum of the M28 *Chandra* source 26 fitted with a NS atmosphere. The best fit model for the pure H atmosphere is reported as a dashed line and the dotted line shows the model without pile-up. Residuals are shown for the initial H atmosphere fit without pile-up and for different chemical compositions.

all five ObsIds, and only froze the ObsId 9132 value to 1. This led to the following best fit values for the normalization of each ObsId with their 90% confidence errors: 0.93 ± 0.08 (2684), 0.89 ± 0.08 (2685), 0.99 ± 0.08 (2683), 1.0 (9132), 0.99 ± 0.05 (9133). The largest deviation is thus at 2.3 sigma (ObsId 2685), still consistent with unity. We performed a similar test with $N_{\rm H}$ and found no significant variability as well. Consequently, we confirm that no significant variability is observed between the different epochs, both in the flux and in the spectral shape.

We also tested for the presence of a hard tail in the X-ray spectrum by adding a power law component. However, the normalization of this component quickly tends to zero, and the fraction of flux in the 0.3–8 keV energy band of this component cannot be higher than 5% or 7% of the total model flux (at the 95% confidence level) for a photon-index of 1.5 and 2.5, respectively.

We performed the same fitting procedure with an atmosphere model composed of pure He (using opacity tables computed by the Opacity Project[3]; see Ho & Heinke 2009 for details), and including the pile-up model. A similar good fit was obtained (χ^2_ν/dof = 0.88/142, see Figure 2) with $N_{\rm H} = (2.65 \pm 0.25) \times 10^{21}$ cm^2, a temperature $kT_{\rm eff} = 170^{+50}_{-90}$ eV, a mass $M = 2.0^{+0.5}_{-1.5}$ $M_\odot$ and a radius $R = 14^{+3}_{-8}$ km. The confidence contours obtained with the *steppar* command are reported in Figure 3 (right). We note that the regions delimited by the contours are not consistent at the 80% confidence level with the contours obtained with the H model.

Finally, we performed a similar fit with a carbon atmosphere model (Ho & Heinke 2009). We obtain an acceptable fit (χ^2_ν/dof = 0.88/142, see Figure 2) but the parameter values are excluded by causality (Rhoades & Ruffini 1974): $M > 2.6$ $M_\odot$ for $R = 10 \pm 2$ km.

[3] http://cdsweb.u-strasbg.fr/topbase/TheOP.html

4 DISCUSSION

The lack of variability of the source over six years agrees with the idea that the target is a LMXB in a quiescent, low-accretion state (e.g. Rutledge et al. 2002b). Such qLMXBs can be X-ray transients with episodes of higher accretion that would heat up the NS star surface to the current observed temperatures (Brown et al. 1998). Such a behavior has been observed for similar sources in GCs (e.g. Rutledge et al. 2002a; Heinke et al. 2003, 2010; Pooley & Hut 2006; Degenaar & Wijnands 2011). It is thus possible that this source becomes suddenly more luminous in the future.

For both a H and a He model, we found good fits with an absorption consistent with the expected absorption from the GC reddening, suggesting that the source is located in the core of M28 with no or very low intrinsic absorption. The mass and radius are as expected for a typical NS (e.g. Lattimer 2010), and the temperature is in the expected range for qLMXBs. No hard tail is observed in the spectrum, which seems to be a common feature of these objects in GCs (Heinke et al. 2003, but see Wijnands et al. 2005).

The only striking difference is that H and He atmosphere models give distinct contour regions of masses/radii at the 80% confidence level (Figure 3). On the one hand, the H model gives a mass and radius consistent with the canonical value of 1.4 $M_\odot$ and 10 km, and allows for the presence of exotic matter inside NSs (hyperons, quarks). On the other hand, the He model provides solutions with higher masses/radii, consistent with the stiffest EOS for NS interiors, most of them composed of neutrons and protons.

The accurate measurement of 1.97 ± 0.04 $M_\odot$ for PSR J1614-2230 (Demorest et al. 2010) does not, by itself, indicate that a H atmosphere is ruled out since there are EOS that have a maximum mass above 2 $M_\odot$ and lie within the H model confidence contours (AP4, but also others not shown in Figure 3; see, e.g., Lattimer 2010; Weissenborn et al. 2011; Massot et al. 2012). The He atmosphere model also allows for several stiff EOS that reach masses higher than 2 $M_\odot$. We note that there are additional sources of error to consider (beyond the statistical uncertainties from spectral fitting) that does not allow for strict constraints on the NS parameters and the EOS, and may slightly enlarge the regions showed in Figure 3. Uncertainties on the distance were not included in our analysis, but this value is relatively well constrained as the source is in a GC. This has no impact when comparing H and He models as the same distance is used for both models. Although pile-up is a small effect and was carefully modeled in the fit, the additional parameters of the pile-up model may introduce additional systematic uncertainties.

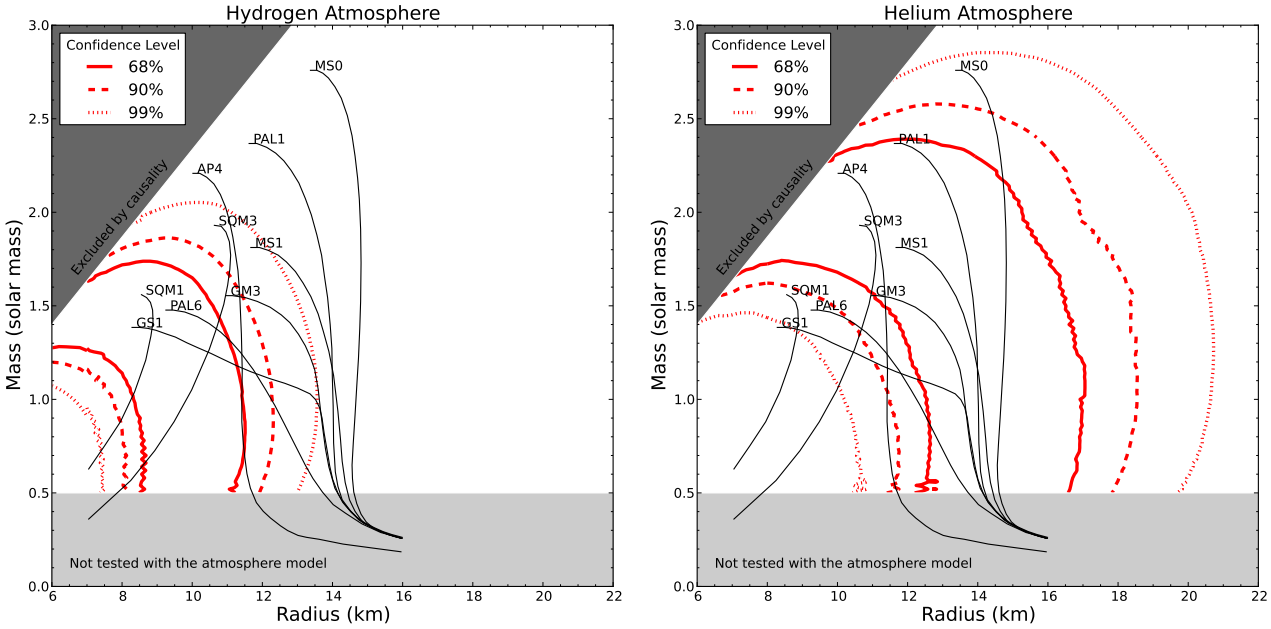

Figure 3. Confidence levels for the mass and radius of the M28 NS *Chandra* source 26, using a H (left) or He (right) atmosphere model. A representative selection of EOS are reported (labelled as in Lattimer & Prakash 2001). The parameters were not allowed to vary in the area "Not tested with the atmosphere model". We report in dark gray the area excluded by causality (Rhoades & Ruffini 1974).

The composition of the NS atmosphere depends on the accreting material, physical processes occurring during the accretion, and conditions on the NS surface. A non-evolved star will produce mostly H, which will quickly stratify to provide a pure H atmosphere. White dwarf donors (in so-called ultra-compact LMXBs) will provide mostly He, C/O, or O/Ne/Mg depending on the white dwarf. Ultra-compact LMXBs are observed to be much more common in GCs than in the rest of the Galaxy (Deutsch et al. 2000). Of 16 bright LMXBs in 13 clusters, we have 11 orbital period measurements, of which 5 indicate ultra-compact systems (e.g. Zurek et al. 2009; Altamirano et al. 2010). In the rest of the Galaxy, only 9 ultra-compact systems are known among the ∼80 bright LMXBs with period measurements (Ritter & Kolb 2003, 2010). Dynamical formation of ultra-compact LMXBs in GC cores explains this difference (Verbunt 1987; Ivanova et al. 2005).

It is unclear whether spallation always produces H during accretion (Bildsten et al. 1992, 1993; Chang & Bildsten 2004). Theoretical work is needed to clarify the conditions for spallation. Obtaining a high-quality X-ray spectrum of an neutron star ultra-compact LMXB in quiescence at known distance would help clarify this question.

Among the qLMXBs in GCs that were used to derive constraints on the mass and radius of their NS using a H atmosphere models, some were reported to have a low mass or radius. For example, the source in the core of NGC 6553 (XMMU J180916255425) gives a NS radius $R_{\rm NS} = 6.3^{+2.3}_{-0.8}$ km for a mass of 1.4 $M_\odot$ (Guillot et al. 2011). The qLMXB in M13 (Gendre et al. 2003a) and the one in NGC 2808 (Servillat et al. 2008b,a) also showed relatively low masses/radii with a radius lower than 10 km or a mass around 1 $M_\odot$ (Webb & Barret 2007; Steiner et al. 2010), however the values are not well constrained. In a same way, the qLMXB U24 in NGC 6397 was reported to show a relatively small radius $R_{\rm NS} = 8.9^{+0.9}_{-0.6}$ km for a mass of 1.4 $M_\odot$ (Guillot et al. 2011). On the other hand, X7 in 47 Tuc was reported with higher values of mass/radius ($R > 12$ km or $M > 2$ $M_\odot$, Heinke et al. 2006), while the NS in ω Cen appears as an intermediate case (Rutledge et al. 2002a; Gendre et al. 2003b), as is the NS studied in this work.

Following our study of the qLMXB in M28, it is possible that some of those sources harbor a NS with a He atmosphere, rather than a H atmosphere. This would favor higher radii and masses for NS, and thus stiffer EOS, in agreement with the precise measurement of relatively high masses for some NS (e.g. ∼2 $M_\odot$, Demorest et al. 2010). We will thus try fitting other quiescent LMXBs with He (and carbon) atmospheres in future work.

Identifying the composition of the atmosphere of known quiescent LMXBs is clearly of key importance, and we suggest three means of doing so. i) Spectroscopy, or (less time-consuming) narrow-filter photometry of optical counterparts can identify Hα emission from LMXBs in quiescence or outburst and thus the presence of H; the LMXB in ω Cen (Haggard et al. 2004) and X4 and X5 in 47 Tuc (van den Berg et al., in prep) therefore possess H atmospheres. ii) Orbital periods differentiate between ultra-compact and longer period systems; we note that long periods are known for X5 and W37 in 47 Tuc (Heinke et al. 2005), suggesting a main-sequence companion and accretion of H. iii) Finally, thermonuclear bursts can distinguish between H-rich and H-poor environments, particularly at low (< 0.01 $\dot{M}_{\rm Edd}$) accretion rates where H should burn unstably (e.g. Fujimoto et al. 1981; Galloway et al. 2008).

This last point is of particular interest for the M28 qLMXB, since a peculiar X-ray burst was observed from this GC (Gotthelf & Kulkarni 1997). This burst was unusually low-luminosity, suggesting burning on only one patch of the

star. The short timescale of this burst (τ=7.5 s) requires He burning without the presence of H, and thus (given the quiescent state) pure He accretion and a pure He atmosphere. Unfortunately we cannot be certain that this burst originated from the known qLMXB, as other qLMXBs may be hidden among the fainter sources in this cluster.

ACKNOWLEDGMENTS

We thank the referee for their careful reading and useful suggestions that strengthened the paper. MS acknowledges supports from NASA/Chandra grant GO0-11063X, NSF grant AST-0909073 and the Centre National d'Etudes Spatiales (CNES). COH is supported by NSERC and an Ingenuity New Faculty Award. WCGH appreciates the use of the computer facilities at KIPAC and acknowledges support from STFC in the UK.

REFERENCES

Alcock C., Illarionov A., 1980, ApJ, 235, 534
Altamirano D., Patruno A., Heinke C. O., Markwardt C., Strohmayer T. E., Linares M., Wijnands R., van der Klis M., Swank J. H., 2010, ApJ, 712, L58
Arnaud K. A., 1996, ADASS V, ASP Conference Series, 101, 17
Becker W., Swartz D. A., Pavlov G. G., Elsner R. F., Grindlay J., Mignani R., Tennant A. F., Backer D., Pulone L., Testa V., Weisskopf M. C., 2003, ApJ, 594, 798
Bildsten L., Salpeter E. E., Wasserman I., 1992, ApJ, 384, 143
Bildsten L., Salpeter E. E., Wasserman I., 1993, ApJ, 408, 615
Bogdanov S., van den Berg M., Servillat M., Heinke C. O., Grindlay J. E., Stairs I. H., Ransom S. M., Freire P. C. C., Bégin S., Becker W., 2011, ApJ, 730, 81
Broos P. S., Townsley L. K., Feigelson E. D., Getman K. V., Bauer F. E., Garmire G. P., 2010, ApJ, 714, 1582
Brown E. F., Bildsten L., Chang P., 2002, ApJ, 574, 920
Brown E. F., Bildsten L., Rutledge R. E., 1998, ApJ, 504, L95
Chang P., Bildsten L., 2004, ApJ, 605, 830
Chang P., Bildsten L., Arras P., 2010, ApJ, 723, 719
Damiani F., Maggio A., Micela G., Sciortino S., 1997, ApJ, 483, 350
Davis J. E., 2001, ApJ, 562, 575
Degenaar N., Wijnands R., 2011, MNRAS, 414, L50
Demorest P. B., Pennucci T., Ransom S. M., Roberts M. S. E., Hessels J. W. T., 2010, Nature, 467, 1081
Deutsch E. W., Margon B., Anderson S. F., 2000, ApJ, 530, L21
Fujimoto M. Y., Hanawa T., Miyaji S., 1981, ApJ, 247, 267
Galloway D. K., Lampe N., 2012, ApJ, 747, 75
Galloway D. K., Muno M. P., Hartman J. M., Psaltis D., Chakrabarty D., 2008, ApJS, 179, 360
Gänsicke B. T., Braje T. M., Romani R. W., 2002, A&A, 386, 1001
Gendre B., Barret D., Webb N., 2003a, A&A, 403, L11
Gendre B., Barret D., Webb N. A., 2003b, A&A, 400, 521
Gotthelf E. V., Kulkarni S. R., 1997, ApJ, 490, L161
Guillot S., Rutledge R. E., Brown E. F., 2011, ApJ, 732, 88
Guillot S., Rutledge R. E., Brown E. F., Pavlov G. G., Zavlin V. E., 2011, ApJ, 738, 129
Haggard D., Cool A. M., Anderson J., Edmonds P. D., Callanan P. J., Heinke C. O., Grindlay J. E., Bailyn C. D., 2004, ApJ, 613, 512
Harris W. E., 1996, AJ, 112, 1487
Harris W. E., 2010, arXiv, 1012, 3224
Heinke C. O., Altamirano D., Cohn H. N., Lugger P. M., Budac S. A., Servillat M., Linares M., Strohmayer T. E., Markwardt C. B., Wijnands R., Swank J. H., Knigge C., Bailyn C., Grindlay J. E., 2010, ApJ, 714, 894
Heinke C. O., Grindlay J. E., Edmonds P. D., 2005, ApJ, 622, 556
Heinke C. O., Grindlay J. E., Lugger P. M., Cohn H. N., Edmonds P. D., Lloyd D. A., Cool A. M., 2003, ApJ, 598, 501
Heinke C. O., Rybicki G. B., Narayan R., Grindlay J. E., 2006, ApJ, 644, 1090
Ho W. C. G., Heinke C. O., 2009, Nature, 462, 71
Ivanova N., Rasio F. A., Lombardi J. C., Dooley K. L., Proulx Z. F., 2005, ApJ, 621, L109
Krauss L. M., Chaboyer B., 2003, Science, 299, 65
Lattimer J. M., 2010, New A, 54, 101
Lattimer J. M., Prakash M., 2001, ApJ, 550, 426
Lattimer J. M., Prakash M., 2010, arXiv, 1012, 3208
Massot É., Margueron J., Chanfray G., 2012, Europhysics Letters, 97, 39002
Özel F., Baym G., Güver T., 2010, Physical Review D, 82, 101301
Pooley D., Hut P., 2006, ApJ, 646, L143
Predehl P., Schmitt J. H. M. M., 1995, A&A, 293, 889
Rhoades C. E., Ruffini R., 1974, Phys. Rev. Lett., 32, 324
Ritter H., Kolb U., 2003, A&A, 404, 301
Ritter H., Kolb U., 2010, VizieR On-line Data Catalog, 1, 02018
Rutledge R. E., Bildsten L., Brown E. F., Pavlov G. G., Zavlin V. E., 2002a, ApJ, 578, 405
Rutledge R. E., Bildsten L., Brown E. F., Pavlov G. G., Zavlin V. E., 2002b, ApJ, 577, 346
Servillat M., Dieball A., Webb N. A., Knigge C., Cornelisse R., Barret D., Long K. S., Shara M. M., Zurek D. R., 2008a, A&A, 490, 641
Servillat M., Webb N. A., Barret D., 2008b, A&A, 480, 397
Steiner A. W., Lattimer J. M., Brown E. F., 2010, ApJ, 722, 33
Testa V., Corsi C. E., Andreuzzi G., Iannicola G., Marconi G., Piersimoni A. M., Buonanno R., 2001, AJ, 121, 916
Verbunt F., 1987, ApJ, 312, L23
Webb N. A., Barret D., 2007, ApJ, 671, 727
Weissenborn S., Sagert I., Pagliara G., Hempel M., Schaffner-Bielich J., 2011, ApJ, 740, L14
Wijnands R., Heinke C. O., Pooley D., Edmonds P. D., Lewin W. H. G., Grindlay J. E., Jonker P. G., Miller J. M., 2005, ApJ, 618, 883
Wilms J., Allen A., McCray R., 2000, ApJ, 542, 914
Zavlin V. E., Pavlov G. G., Shibanov Y. A., 1996, A&A, 315, 141
Zurek D. R., Knigge C., Maccarone T. J., Dieball A., Long K. S., 2009, ApJ, 699, 1113